Derivation and validation of estimation model of rainfall kinetic energy under canopy

Zixi Li[1], Fuqiang Tian[1]

[1]Department of Hydraulic Engineering, State Key Laboratory of Hydroscience and Engineering, Tsinghua University, Beijing 100084, China

Correspondence to: Fuqiang Tian (tianfq@tsinghua.edu.cn)

Abstract. The interception effect of the canopy on rainfall alters the kinetic energy of the rainfall as it reaches the ground, which is crucial for soil and water conservation, ecosystem stability, and energy transfer within environmental systems. A novel estimation model for the kinetic energy of rainfall under canopy is developed by stratifying the canopy using parameters such as leaf area index and leaf inclination angle, explicitly distinguishing between canopy-dripped and splashed raindrops. The efficacy of the model is subsequently assessed and analyzed through a comprehensive examination of nine field datasets encompassing LiDAR and raindrop spectrum observations. The simulated under-canopy total kinetic energy, splashing drop kinetic energy, and dripping drop kinetic energy showed total R^2 values of 0.769, 0.572 and 0.773, total RMSE values of 18.7, 2.0 and 18.7 J m^{-2} h^{-1}, with measurement including uncertainty of 54.1±12.4, 3.7±0.1 and 50.4±12.4 J m^{-2} h^{-1}, respectively. Simulations indicate that the sub-canopy raindrop spectrum and kinetic energy are mainly governed by canopy physical properties and remain relatively stable despite variations in above-canopy rainfall. Sensitivity analysis shows that the model is generally robust, with rainfall intensity, the pinning proportion coefficient, LAI and surface contact angle exerting the greatest influence, while other factors have limited impact. Remaining limitations, including simplified branch-drip representation, component-partitioning assumptions and measurement uncertainties, highlight the need for improved parameterization and broader observations.

1. Introduction

Canopy interception of rainfall can change both the amount of water amount reaching the ground and the kinetic energy of rainfall, which plays a pivotal role in shaping the hydrological dynamics and ecological integrity of watersheds (Howard, 2022; Momiyama, 2023; Li et al., 2025). The interaction between raindrops and the canopy, encompassing processes such as collision, splashing, and dripping, alters the kinetic energy of rainfall as it reaches the ground. The kinetic energy of rainfall is a crucial parameter with significant implications for soil and water

conservation, ecosystem stability, and energy transfer within environmental systems. (Montero-Martínez et al., 2020). The influence of the canopy on sub-canopy kinetic energy is complex and not easily assessed, despite its importance for soil and water conservation (Brasil et al., 2022; Nanko et al., 2013; Nanko, Mizugaki et al., 2008). Canopy effects depend on vegetation type and physical traits such as leaf area index, leaf orientation, and canopy height (Geißler et al., 2013; Pflug et al., 2021; Tu et al., 2021; Zhang et al., 2023). Larger raindrops tend to break into smaller droplets, reducing kinetic energy (Alivio et al., 2023; Senn et al., 2020), while interception can form larger drops and decrease drop number, broadening the distribution and increasing kinetic energy beneath the canopy (Nanko, Onda et al., 2008; Katayama et al., 2023; Zhang et al., 2021).

Understanding these complex canopy-rainfall interactions is essential for accurately estimating sub-canopy kinetic energy. However, due to the inherent variability in raindrop size, velocity, and canopy structure, most studies have relied on experimental measurements to quantify kinetic energy, while relatively few modeling approaches have been developed. The experimental measurement method includes sample cup model, funnel model (Van Dijk et al., 2002) and filter paper dyeing method (Li et al., 2019). While the emerging laser raindrop spectrometer can measure the size and velocity distribution of raindrops more precisely (Fernández-Raga et al., 2010), which facilitates the study of rainfall kinetic energy. Some scholars also use remote sensing methods (Senn et al., 2020; Miralles et al, 2010) to simulate the kinetic energy of rainfall over a large area.

Most existing model for estimating understory kinetic energy are to perform simple function fitting on understory kinetic energy and parameters such as rainfall intensity or canopy height. These methods are highly empirical and have poor adaptability to canopies of different types and properties (Brandt, 1990; Li et al., 2019). Some scholars have considered combining the physical motion processes of raindrops falling and splashing to analyze raindrop size distribution under the canopy, but a simple and effective simulation model has not yet been established (de Moraes Frasson and Krajewski, 2013; Murakami, 2021).

Recent studies have investigated the partitioning of rainfall beneath the canopy into splash, stem drip, and free throughfall, evaluating how rainfall characteristics and canopy traits influence each component (Levia et al., 2019; Nanko et al., 2022; Nanko et al., 2025). These findings provide a mechanistic basis for developing models to estimate sub-canopy kinetic energy by component. In addition, Li and Tian (2025) and Li et al. (2025) approached the problem from the microscopic processes of raindrop movement within the canopy, establishing models to estimate canopy interception. Such modeling approaches offer valuable guidance for building predictive frameworks that integrate both physical mechanisms and component partitioning to simulate sub-canopy kinetic energy.

Despite advances in experimental measurements and modeling, accurately estimating sub-canopy kinetic energy remains challenging. Existing models are largely empirical and poorly adaptable across canopy types, and while rainfall partitioning studies provide a mechanistic basis, they are rarely integrated into predictive models. This study aims to develop a novel model for quantitatively estimating sub-canopy kinetic energy, incorporating rainfall component partitioning and the microphysical behavior of raindrops within the canopy based on canopy physical parameters. The model derivation is presented in Sect. 2, followed by model validation and sensitivity analysis in Sect. 3, while Sect. 4 discusses the model limitations and future work.

2. Influence of canopy on rainfall energy and model derivation

2.1 Influence of canopy on rainfall energy

The canopy physical function in the interception process involves altering the kinetic energy of raindrops, by changing their size and velocity, while also capturing a portion of the incoming rainfall. The Rutter model (Levia et al., 2011; Valente and Gash, 1997; Rutter et al., 1971; Gash and Morton, 1978) illustrates a traditional canopy interception process for rainfall, as depicted in Figure 1. A segment of the rainfall is initially captured by the leaves, with droplets commencing their descent once the leaf surface is saturated. Concurrently, another portion is retained by the stems, which, following interception and retention, is transported to the ground as stem flow. Throughout the rainy period, both stems and leaves are subject to evaporation.

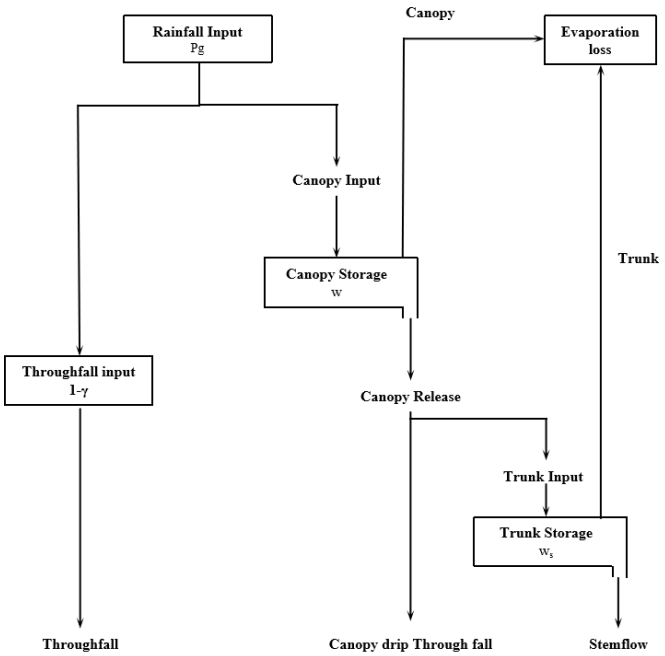

(a) Original canopy interception processes

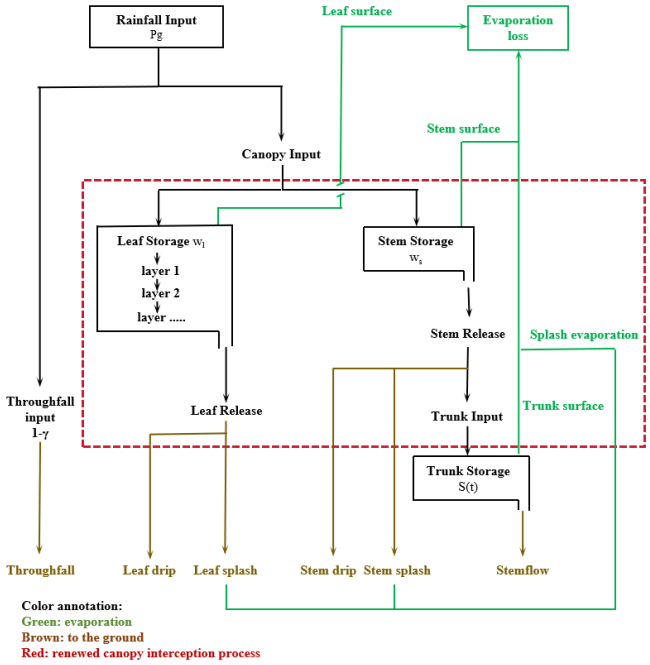

(b) Refined canopy interception processes

Figure 1. (a) Original canopy interception processes (adapt from Gash and Morton (1978), Valente and Gash (1997)); (b) Refined canopy interception processes. The section demarcated by the red dashed lines represents the enhanced portion of the flowchart as compared to the original Rutter model. The primary modifications entail a distinct separation of the interception processes for stems and leaves, acknowledging that the stem area index of certain canopies is substantial, rendering the interception capacity of stems non-negligible (Xiao et al., 2000). Additionally, the updated flowchart incorporates the splash process and the subsequent evaporation of splash droplets from both stems and leaves.

Previous observations and research (Li and Tian, 2025; de Moraes Frasson and Krajewski, 2013) indicate that the canopy interception flow diagram proposed by Rutter et al. (1971) remains insufficient in capturing the comprehensive physical dynamics and kinetic energy of raindrops. Beyond the canopy drip phenomenon illustrated in Figure 1 (a), raindrops are also subject to breakage and splashing upon collision with the canopy, which plays an important role in kinetic energy change of droplets. This splashing phenomenon is crucial for accurately depicting the canopy interception effect on rainfall (Murakami, 2021). Consequently, there is a need to refine the canopy interception process based on the Rutter flow diagram.

The revised canopy interception process is depicted in Figure 1 (b). From a component perspective, raindrops penetrating the canopy can be classified into three types: free throughfall, splash throughfall, and canopy drip (Levia et al., 2017). In Figure 1 (b), for the rainfall intercepted by leaves, the collision process results in two distinct forms of raindrops: splashed drops and canopy drips. Regarding the interception by stems, the impact of raindrops against

the stem leads to some splashing or dripping, while another portion is retained by the stem, eventually contributing to stem flow once the stem is saturated. Given that the velocity of stem flow is significantly slower than that of raindrops falling directly from the sky, some water is retained during this process and the kinetic energy of stem flow is not taken into account. Moreover, evaporation occurs from the splashed drops on both leaves and stems, which, combined with surface evaporation, forms the total rainy season evaporation. Concurrently, water between leaves and stems may interchange during splashing and dripping. However, due to the minimal volume of this water, it is not accounted for in Figure 2 nor in subsequent modeling analyses.

2.2 Model derivation

The core principle of rainfall kinetic energy estimation is to estimate the size and speed of raindrops under the canopy based on the physical and structural properties. The derivation of this model is based on the work of Li et al. (2025) and Li and Tian (2025).

Since the shape of a raindrop is not an ideal sphere, the equivalent diameter D (mm) of the raindrop is usually used instead. Therefore, kinetic energy E(D) (J) can be calculated according to the following equation:

$$E(D) = \frac{\pi \rho D^3 {v_0}^2}{12} \quad (1)$$

where, v_0 is the fall velocity (m/s), ρ is the density of water, which is 1.0×10^{-6} kg/mm^3 under standard conditions. Therefore, the total kinetic energy E_{K_total} (J) can be directly substituted into the simulated raindrop spectrum, such as the gamma function raindrop spectrum, or into the real raindrop spectrum, such as the raindrop spectrum measured by the drop spectrometer:

$$E_{K\_total} = \sum_{i=1}^{N} E(D_i) \quad (2)$$

Then, calculate the kinetic energy per unit area and unit rainfall depth E_{Kp} (J m^{-2} mm^{-1}):

$$E_{Kp} = \frac{E_{K\_total}}{P \times A} \quad (3)$$

where, A is the drop spectrometer observation area (54cm^2), P is the amount of rainfall (mm). The total kinetic energy of rainfall per unit area per unit time E_K (J m^{-2} h^{-1}) is:

$$E_K = \frac{E_{K\_total}}{A \times t_0} = E_{Kp} \times I \quad (4)$$

where, t_0 is the drop spectrometer observation time (h).

Therefore, the corresponding kinetic energy of rainfall under the canopy E_{K_in} (J m^{-2} h^{-1}) is:

$$E_{K\_in} = (1-\gamma) \cdot E_{K\_out} + E_s + E_d \quad (5)$$

where, γ is the fractional vegetation cover (FVC), E_{K_out} is the kinetic energy of rainfall outside the canopy (J m^{-2} h^{-1}), $(1-\gamma)\cdot E_{K\_out}$ is the free throughfall kinetic energy (J m^{-2} h^{-1}), E_s is the splash drop kinetic energy (J m^{-2} h^{-1}), and E_d is the canopy drip kinetic energy (J m^{-2} h^{-1}).

The volume distribution of raindrops contributing to free throughfall is the same as that outside the canopy. For splashed droplets, the particle size is mainly distributed between 0.3 and 1.3 mm shown in Figure 5, and their volume distribution can be referenced from the Weibull distribution proposed by Levia et al. (2019) for droplets in the 1-2 mm range. To unify the volume distribution of splashed droplets both ≤1 mm and 1-2 mm and to simplify the modeling, this study approximates their volume distribution using a triangular distribution with a peak at 0.8 mm and zero values at 0.3 mm and 1.3 mm.

For raindrops attached to leaves, canopy drip can be divided into dripping raindrops and sliding raindrops according to their movement form. The sizes of the two can be calculated using the following formula (Konrad et al., 2012, Li et al., 2025):

$$s_{max} = l\cdot\frac{(1+cos\theta)}{\sqrt{2+cos\theta}}\cdot\sqrt{\frac{1\cdot sinX}{\pi}},\ l=\sqrt{\frac{6\sigma}{\rho}}\cdot\sqrt{\frac{1}{g\cdot sin\alpha+k{v_w}^2}}$$

when $tan\alpha > \frac{2}{\pi}tanX$, the droplet will slip

$$s_{max} = l\cdot\frac{(1+cos\theta)}{\sqrt{2+cos\theta}}\cdot\sqrt{\frac{sin\alpha\cdot cosX}{2\cdot cos\alpha}} \quad (6)$$

when $tan\alpha < \frac{2}{\pi}tanX$, the droplet will drip

where s_{max} (mm) is the maximum radius of the droplet contact surface, θ is the average of the advancing and retreating contact angles on the leaf surface, X is half of the difference between the front and rear contact angles, α is the leaf inclination angle of the canopy, k is a coefficient that reflects wind load effect and determined by experiment, which can be selected 0.09 (Li et al., 2025), σ is the surface tension coefficient of water which can be taken as 7.2×10^{-2} N/m, v_w is the wind speed (m/s). Therefore, Eqs (6) accounts for the effect of wind load on raindrop size. In subsequent analyses, the term "canopy drip" is used to replace the two physical processes of "slip droplet" and "drip droplet" for the purpose of analysis. The volume of a single drip droplet is:

$$V=\frac{\pi s^3}{3}\frac{(1-cos\theta)^2(2+cos\theta)}{sin^3\theta} \quad (7)$$

where s (mm) is radius of the droplet contact surface. The volume distribution of the canopy drip can be derived based on the leaf inclination angle distribution function $f(\alpha)$ and Eqs (6) and (7) (Li and Tian, 2025). The radius of

canopy drip is computed using Eqs (6). For a given tree, leaf inclination angle is the only parameter in Eqs (6) that varies among leaves, while the remaining parameters remain constant. Leaves with larger inclination angles produce canopy drip of smaller radius, and vice versa. Therefore, the radius distribution of canopy drip can be derived from the probability distribution function of leaf inclination angles, and the corresponding volume distribution can then be obtained using Eq (7). It is worth noting that this model assumes the same model for calculating stem interception (Li et al., 2025), as well as identical volume distribution functions for stem-generated splash droplets and stem drip as those used for leaves. The implications of this assumption are discussed in the Sect. 4.

The droplet velocity can be determined based on Atlas et al (1973). and Mou (1983) research:

$$v = \begin{cases} 0.496 \times 10^{\sqrt{28.32+6.524lg0.1D-(lg0.1D)^2}-3.665}, & D < 0.6\ mm\ (\text{Mou}, 1983) \\ v = 9.65 - 10.3 \times e^{-0.6D}, & D > 0.6\ mm\ (\text{Atlas et al.}, 1973) \end{cases} \quad (8)$$

where, D is the raindrop diameter (mm) and v is the final velocity of the droplet (m/s). Since the formula by Atlas et al. (1973) is applicable to raindrops of 0.6–5.8 mm in diameter, the formula by Mou (1983) was adopted for diameters below 0.6 mm. At the transition diameter of 0.6 mm, the terminal velocities given by the two formulas are 2.46 m s^{-1} (Atlas et al., 1973) and 2.36 m/s (Mou, 1983), respectively, differing by only 0.1 m s^{-1}. This discrepancy at the breakpoint is considered acceptable. When the water drop comes from height h (m), its velocity is (Yao and Chen, 1993):

$$v_{\_in} = v \times (1 - e^{\frac{-2gh}{v^2}})^{\frac{1}{2}} \quad (9)$$

where h is the falling height (m) and $v_{\_in}$ is the raindrop velocity inside the canopy (m/s). In the actual canopy, the height h can be taken as the middle height value of the last canopy layer.

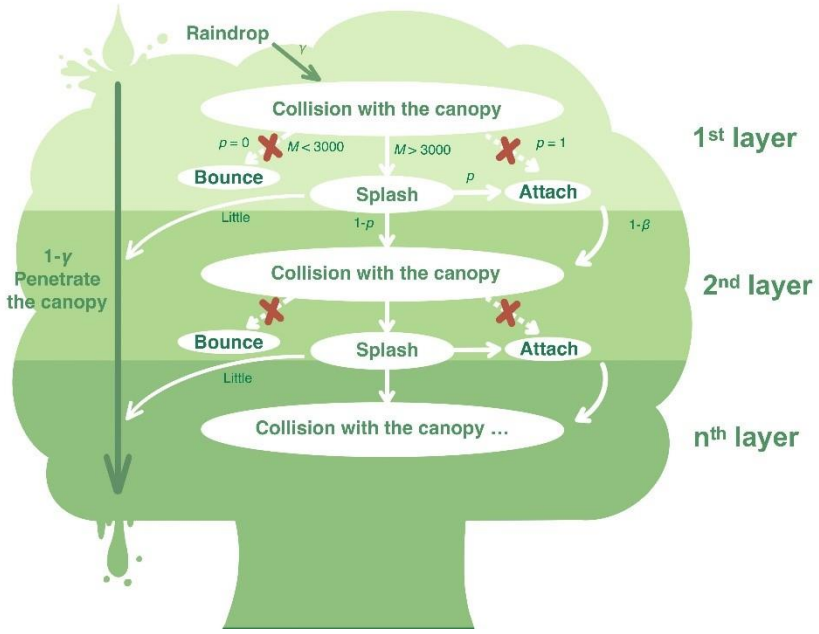

Figure 2. The theoretical canopy interception model based on raindrop microphysical processes raised by Li and Tian (2025).

According to the splash theory and the model of canopy interception microphysical process shown in Figure 2 (Li and Tian, 2025), the ratio of splashing droplets and canopy drip depends on the collision process of the last canopy. if there are $\frac{LAI \cdot G}{\gamma}$ leaf layers, assuming that the saturation level of each leaf layer is consistent and equal to $\frac{w_l}{Y}$, where w_l is the leaf interception volume (mm) and Y is leaf interception capacity (mm). Considering the splash of stems and leaves at the same time, the amount of water reaching the last canopy layer I' (mm/h) is:

$$I' = I \times \left[\gamma(1-p_t) \times (1-\beta p)^{\frac{LAI \cdot G}{\gamma}-1} + K_l \frac{w_l}{Y} + p_t \gamma\right]$$
$$K_l = \gamma[1-(1-\beta p)^{\frac{LAI \cdot G}{\gamma}-1}](1-p_t) \quad (10)$$

where, γ is FVC, G is the leaf area projection ratio, p is pinning proportion coefficient which is defined as the proportion remaining on the leaf or stem after splashing, and then $(1-p)$ is the proportion of splashed water droplets, β is attachment retention coefficient which is defined as a proportion that remains permanently on the leaf without dripping, $p_t = \frac{SAI}{LAI+SAI}$ is stem area proportion. In the equations (11), $\left[\gamma(1-p_t) \times (1-\beta p)^{\frac{LAI \cdot G}{\gamma}-1}\right]$ describes the proportion that is not intercepted by the leaves, $\left[K_l \frac{w_l}{Y}\right]$ represents the proportion of leaf drip due to saturation, and $[p_t \gamma]$ describes the proportion of raindrops colliding with the stem (assuming that the stem only has one layer). The leaf interception volume w_l is calculated based on the simplified model form raised by Li and Tian (2025).

Therefore, the volumetric proportion of leaf and stem splash drops is:

$$k_s = (1-p) \times \left[\gamma(1-p_t) \times (1-\beta p)^{\frac{LAI \cdot G}{\gamma}-1} + K_l \frac{w_l}{Y} + p_t \gamma\right] \quad (11)$$

the volumetric proportion of canopy drip including leaf and stem drip is:

$$k_a = p \times \left[(1-\beta)\gamma(1-p_t) \times (1-\beta p)^{\frac{LAI \cdot G}{\gamma}-1} + K_l \frac{w_l}{Y} + \gamma p_t D_d \times \frac{w_s}{S}\right] \quad (12)$$

where, D_d is defined as the proportion of canopy drip in the stem flow, w_s is the stem interception volume (mm), S is the stem interception capacity (mm). The splash droplet mass m_s and canopy drip mass m_a per unit area per unit time (kg m^{-2} h^{-1}) are:

$$\begin{aligned} m_s &= \rho \times I \times k_s \\ m_a &= \rho \times I \times k_a \end{aligned} \quad (13)$$

At last, E_{K_in} (J m^{-2} h^{-1}) is:

$$E_{K\_in} = (1-\gamma) \cdot E_{K\_out} + \frac{1}{2}\int dm_s {v_s}^2 + \frac{1}{2}\int dm_a {v_a}^2 \quad (14)$$

In summary, the simulation calculation steps of the kinetic energy under canopy are as follows: first calculate the canopy drip volume distribution according to Eqs (6) and (7), then calculate the landing speed of raindrops of different sizes according to Eq (9), then calculate the splash drop and canopy drip mass per unit area per unit time according to Eqs (10-13) , and finally calculate the kinetic energy of raindrops per unit area per unit time under the canopy according to Eq (14) (J m^{-2} h^{-1}) .

The influence of wind load and rainfall intensity will cause changes in the canopy interception capacity. After the rainfall, droplets will still drip due to leaf vibration, generating dripping kinetic energy, which is generally manifested as the hysteresis effect of the understory kinetic energy. In order to better simulate the real-time rainfall kinetic energy intensity, this model allocates the changes in the canopy interception capacity caused by factors such as wind load to a total of 20 minutes after this rainfall period in a ratio of 0.9 and 0.1 in units of 10 minutes to describe the hysteresis effect of the understory kinetic energy.

The estimation model of rainfall kinetic energy under canopy can be summarized as Table 1.

Table 1. Summary of the model of rainfall kinetic energy under canopy

Model variables	Model form
Leaf interception (mm) (Li and Tian, 2025)	$\frac{IK_lY}{IK_l+e_{pl}}\left[1-e^{-\left(\frac{IK_l+e_{pl}}{Y}\right)t}\right]$ $K_l = \gamma[1-(1-\beta p)^{\frac{LAI \cdot G}{\gamma}}](1-p_t)$

Stem interception (mm) (Li and Tian, 2025)	$\frac{IK_sS}{IK_s+e_{ps}}\left[1-e^{-\left(\frac{IK_s+e_{ps}}{S}\right)t}\right]$ $K_s=\gamma\times p_t$
Stem dripping (mm/h)	$I\times K_s\times D_d\times\frac{w_s}{S}$
Stem splashing (mm/h)	$Ip_t\gamma\times(1-p)$
Leaf dripping (mm/h)	$I\times p\times\left[(1-\beta)\gamma(1-p_t)\times(1-\beta p)^{\frac{LAI\cdot G}{\gamma}-1}+K_l\frac{w_l}{Y}\right]$
Leaf splashing (mm/h)	$I\times(1-p)\times\left[\gamma(1-p_t)\times(1-\beta p)^{\frac{LAI\cdot G}{\gamma}-1}+K_l\frac{w_l}{Y}\right]$
Raindrop velocity under canopy (m/s)	$v=\begin{cases}0.496\times10^{\sqrt{28.32+6.524lg0.1D-(lg0.1D)^2}-3.665}, & D<0.6\ mm\ \text{(Mou, 1983)}\\ v=9.65-10.3\times e^{-0.6D}, & D>0.6\ mm\ \text{(Atlas et al., 1973)}\end{cases}$ $v_{\_in}=v\times(1-e^{\frac{-2gh}{v^2}})^{\frac{1}{2}}$
Free throughfall energy (J/m²h)	$(1-\gamma)\cdot E_{K\_out}$
Splash kinetic energy (J/m²h)	$\frac{1}{2}\int dm_s\,{v_s}^2$ $m_s=\rho\times I\times k_s$ $k_s=(1-p)\times\left[\gamma(1-p_t)\times(1-\beta p)^{\frac{LAI\cdot G}{\gamma}-1}+K_l\frac{w_l}{Y}+p_t\gamma\right]$
Canopy drip kinetic energy (J/m²h)	$\frac{1}{2}\int dm_a\,{v_a}^2$ $m_a=\rho\times I\times k_a$ $k_a=p\times\left[(1-\beta)\gamma(1-p_t)\times(1-\beta p)^{\frac{LAI\cdot G}{\gamma}-1}+K_l\frac{w_l}{Y}+\gamma p_t D_d\times\frac{w_s}{S}\right]$

Note: the parameter annotation can be seen in Notation Section.

3. Experimental validation and analysis

3.1 Canopy experimental method

To assess the model simulation efficacy, this research conducted observations of nine rainfall events on *Aesculus chinensis Bunge*, which had a height of 12.8 m, a diameter at breast height (DBH) of 23.3 cm and a clear bole height of 4.1 m, within the Tsinghua University campus. For raindrop spectrum observations, two OTT Parsivel² laser spectrometer were utilized, capable of dividing particle size and velocity into 32 bins, totaling 1024 combinations, with a size range of 0.0625 mm to 24.5 mm and a velocity range of 0.05 to 20.8 m/s. It should be noted that both size and fall-velocity measurements are subject to uncertainties introduced by the instrument's non-uniform binning scheme, and subsequent analyses use the midpoint of each bin as the representative value. One of the laser

spectrometers was situated under a *Aesculus chinensis Bunge* (116.3°E, 40.0°N), while the other was mounted on the roof of Tsinghua University sediment laboratory, approximately 150 meters away, assumes similar rainfall characteristics.

As an effective means of observation, LiDAR has been widely used in the observation and analysis of vegetation structural parameters in recent years (Wang et al., 2023; Mostafa et al., 2022). In this study, Rigel VZ600i ground-based radar was used to observe and extract canopy parameters. Its ranging accuracy was 5 mm within 100 m and the scanning angle accuracy was 0.0028°. The FVC (Fraction of Vegetation Cover) is obtained from the voxel void statistics in the vertical direction. The leaf area density was calculated using the VCP algorithm based on contact frequency (Chen et al., 2024; Hosoi and Omasa, 2006), and then the LAI was obtained by integration along the vertical direction. The leaf inclination angle distribution was calculated using the principal component analysis method based on the leaf normal vector (Maćkiewicz and Ratajczak, 1993) shown in Figure 3 (a). The stem area index and stem inclination angle parameters were extracted based on the branch reconstruction algorithm (Du et al., 2019), and the leaf area projection ratio G can be calculated according to the leaf inclination distribution.

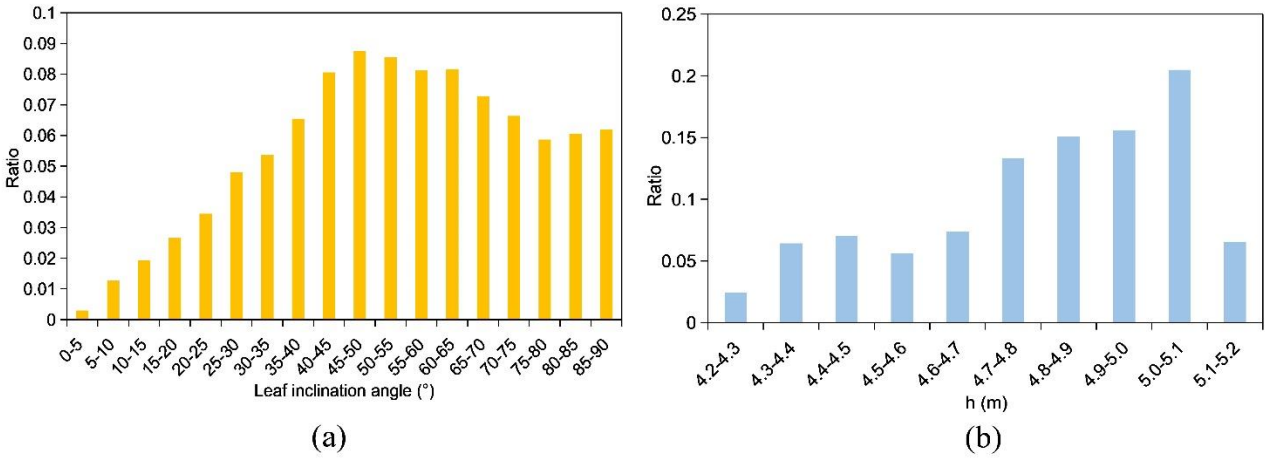

Figure 3. (a) Leaf area proportions across different leaf inclination angle classes; (b) Leaf area proportions across height classes of the lowest leaf layer (drip-capable leaves).

The distribution of drip-capable heights, shown in Figure 3(b), was derived from LiDAR point-cloud data by identifying the first leaf or stem surface encountered when searching upward from the ground. During model computation, the median value of each bin was used as the representative value for that range.

The model parameters under field experimental conditions need to be determined, as shown in Table 2. The observation dates, rainfall duration, accumulated rainfall, mean wind speed and mean rainfall intensity are shown in Table 3. The measured splashing and canopy-drip components were classified based on a droplet-diameter threshold:

after excluding free throughfall, droplets smaller than 1.3 mm were categorized as splashing drops, whereas those larger than 1.3 mm were classified as canopy drip (Levia et al., 2019). It is worth noting that evaporation during rainfall is minimal (Li et al., 2025); therefore, evaporation of leaf and stem is neglected in the following analysis.

Table 2. Parameters of estimation model of rainfall kinetic energy under canopy

Symbol	Method for determining values	Typical Value	Physical meaning	Unit
$f(\alpha)$	Measured by LiDAR	Distribution function (Figure 3 (a))	Leaf inclination distribution	–
G	Calculated by $f(\alpha)$	0.59	Leaf area projection coefficient	–
γ	Measured by LiDAR	0.976	FVC	–
LAI	Measured by LiDAR	10.67	Leaf area index	–
SAI	Measured by LiDAR	1.26	Stem area index	–
h	Measured by LiDAR	4.85 or distribution function (Figure 3 (b))	Falling height of the droplets	m
θ	Measured, Refer to Li et al. (2025)	28	Average of the advancing and retreating contact angles on the leaf surface	°
X	Measured, Refer to Li et al. (2025)	14	Half of the difference between the advancing and receding contact angles	°
k	Fitted from experimental data in Li et al. (2025)	0.09	Wind load effect coefficient	–
p	Fitted from experimental data in Li and Tian (2025), analyzed by sensitive analysis in Sect. 3.3	0.7	Pinning proportion coefficient	–
β	Fitted from experimental data in Li and Tian (2025), analyzed by sensitive analysis in Sect. 3.3	0.9	Attachment retention coefficient	–
D_d	Assumed, analyzed by sensitive analysis in Sect. 3.3	0.6	Proportion of canopy drip in the stem flow	–
Y	Calculated, Refer to interception capacity model (Li et al., 2025)	–	Leaf interception capacity	mm
S	Calculated, Refer to interception capacity model (Li et al., 2025)	–	Stem interception capacity	mm
w_l	Calculated, Refer to interception model (Li and Tian, 2025)	–	Leaf interception volume	mm
w_s	Calculated, Refer to interception model (Li and Tian, 2025)	–	Stem interception volume	mm

225

Table 3. Rainfall characteristics in the experiments

Observation time	duration(min)	Accumulated rainfall (mm)	Wind speed (m/s)	Rainfall intensity (mm/h)

2024.6.25	60	5.72	0.6	5.42
2024.6.29	100	5.28	1.1	3.17
2024.7.1	70	8.51	0.1	6.96
2024.7.19	60	7.45	8.4	7.65
2024.7.25	210	7.05	3.8	2.01
2024.7.29	140	4.73	2.0	2.03
2024.8.20	50	4.63	4.3	5.56
2024.8.25	80	4.94	6.4	3.71
2024.8.26	230	6.71	1.9	1.75

3.2 Model Validation

This section evaluates and analyzes the performance of the understory kinetic energy estimation model by integrating raindrop spectrum observation data of *Aesculus chinensis Bunge* on nine field rainfall events.

230 **Table 4. R^2 and RMSE Performance Metrics for Canopy Rainfall Kinetic Energy Partitioning**

Observation time	Total kinetic energy under canopy				Splash drop kinetic energy under canopy				Drip kinetic energy under canopy			
	R^2	RMSE (J m-2 h-1)	Measurement and uncertainty (J m-2 h-1)	M/O ratio	R^2	RMSE (J m-2 h-1)	Measurement and uncertainty (J m-2 h-1)	M/O ratio	R^2	RMSE (J m-2 h-1)	Measurement and uncertainty (J m-2 h-1)	M/O ratio
2024.6.25	0.683	26.0	92.5±18.1	1.15	0.821	1.9	6.3±0.1	1.08	0.654	28.7	86.2±18.1	1.15
2024.6.29	0.798	13.4	49.4±9.9	1.34	0.406	2.5	3.4±0.1	0.74	0.776	14.5	46.0±9.9	1.36
2024.7.1	0.736	36.1	137.9±21.4	1.09	0.799	3.3	9.5±0.2	0.65	0.744	35.5	128.4±21.4	1.12
2024.7.19	0.680	43.4	151.2±24.8	0.89	0.642	5.1	12.3±0.3	1.18	0.673	42.8	138.9±24.7	0.88
2024.7.25	0.901	3.8	31.8±7.9	1.51	0.535	0.6	1.7±0.0	0.92	0.893	4.0	30.1±7.9	1.51
2024.7.29	0.701	8.6	28.7±5.8	1.17	0.196	1.1	1.6±0.1	0.79	0.729	7.8	27.6±5.8	1.18
2024.8.20	0.794	27.5	83.4±19.2	0.86	0.805	2.3	5.7±0.1	0.61	0.716	28.7	77.7±19.2	0.84
2024.8.25	0.882	15.0	57.3±10.7	0.97	0.792	1.4	4.9±0.1	1.45	0.879	14.1	52.4±10.7	0.96
2024.8.26	0.723	8.4	23.5±6.7	1.40	0.312	0.5	1.4±0.0	1.21	0.742	7.3	22.1±6.7	1.41
Total	**0.769**	**18.7**	**54.1±12.4**	**0.90**	**0.572**	**2.0**	**3.7±0.1**	**1.35**	**0.773**	**18.7**	**50.4±12.4**	**0.87**

Note: The R^2, RMSE and modeled/observed mean ratio metrics for the simulated under-canopy total kinetic energy, splashing drop kinetic energy, and dripping drop kinetic energy (J m^{-2} h^{-1}) derived from these nine rainfall events. The RMSE and R^2 metrics were computed at a 10-min time step in each rainfall event. The measured data refer to the mean value across all observation points for each event. The measurement uncertainty for a rainfall event was estimated by propagating the per-bin uncertainties through all observations and aggregating them over the entire event. The M/O ratio is defined as the modeled mean divided by the observed mean, and it serves as an indicator of the model's prediction bias. The "Total" values were obtained by concatenating the nine rainfall events into a single long sequence to calculate the performance metrics and uncertainty.

The total R^2 values were 0.769, 0.572, and 0.773, and the total RMSE values were 18.7, 2.0 and 18.7 J m^{-2} h^{-1}, with measurement and uncertainty of 54.1±12.4, 3.7±0.1 and 50.4±12.4 J m^{-2} h^{-1} respectively. For drip kinetic energy and total kinetic energy, the measurement uncertainty is already close to the RMSE, indicating that the model performance approaches the observational precision limit. The simulation of under-canopy dripping kinetic energy demonstrated higher accuracy than that of splashing kinetic energy, likely due to the greater complexity and higher uncertainty associated with the splashing phenomenon which is shown in Figure 4. Table 4 also shows that the splash kinetic energy tends to be overestimated, while the drip kinetic energy is generally underestimated, likely because certain components such as stemflow drip points (Nanko et al., 2022) were not considered.

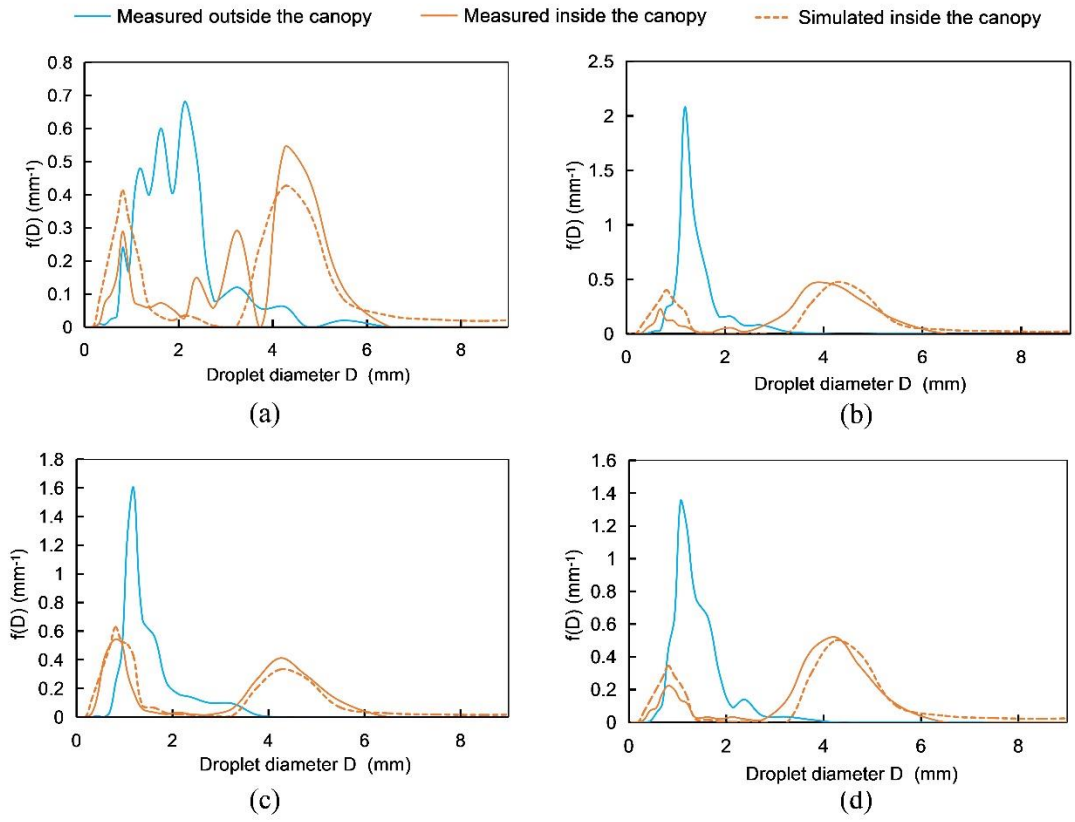

Figure 4. Comparison of raindrop spectra outside the canopy and inside the canopy during two rainfall events. f(D) is the

volumetric drop-size distribution function (Volume fraction per millimeter (mm^{-1})), plotted based on the volume-based frequency. (a) Raindrop spectrum of 0-10 min rainfall on 8.20 (b) Raindrop spectrum of 30-40 min rainfall on 8.20 (c) Raindrop spectrum of 0-10 min rainfall on 8.26 (d) Raindrop spectrum of 150-160 min rainfall on 8.26. The OTT Parsivel² laser spectrometer uses a non-uniform binning scheme to represent drop size distributions. The full diameter range (0.0625-24.5 mm) is divided into 32 classes with variable bin widths: 0.125 mm for D < 1.25 mm, 0.25 mm for 1.25-2.5 mm, 0.5 mm for 2.5-5.0 mm, and 1.0 mm for D > 5.0 mm. The figure is plotted using the midpoint of each bin as the representative value.

Taken rainfall events on 8.20 and 8.26 as examples, the raindrop spectrum data collected beneath the canopy reveals a trend of relative consistency between the measured and simulated raindrop sizes, which is shown in Figure 4. Raindrops smaller than approximately 1.5 mm, which are primarily responsible for splashing (Levia et al., 2017), constitute approximately 10%-30% of the mass ratio. The proportion of measured raindrops within the splashing size range is relatively lower than that of the simulation. Over time, as canopy saturation increases, the relative frequency of splashing drops in both measured and simulated data decreases, while the proportion of dripping raindrops rises. This behavior is consistent across both datasets and aligns with the physical expectation that higher canopy saturation leads to greater canopy drip intensity. Figure 4 also suggests that the canopy exerts an aggregating effect on the kinetic energy of rainfall, indicating that for canopies with similar physical structures, the raindrop spectrum and distribution under the canopy remain relatively stable regardless of variations in the external raindrop spectrum. Based on the analysis in Sect 2.2., this phenomenon occurs because the sub-canopy raindrop spectrum (excluding direct throughfall) is primarily governed by canopy physical parameters such as leaf area index, leaf inclination angle, and leaf contact angle, through raindrop interactions including splashing, dripping, and coalescence within the canopy. This observation is consistent with the findings of Nanko et al. (2025).

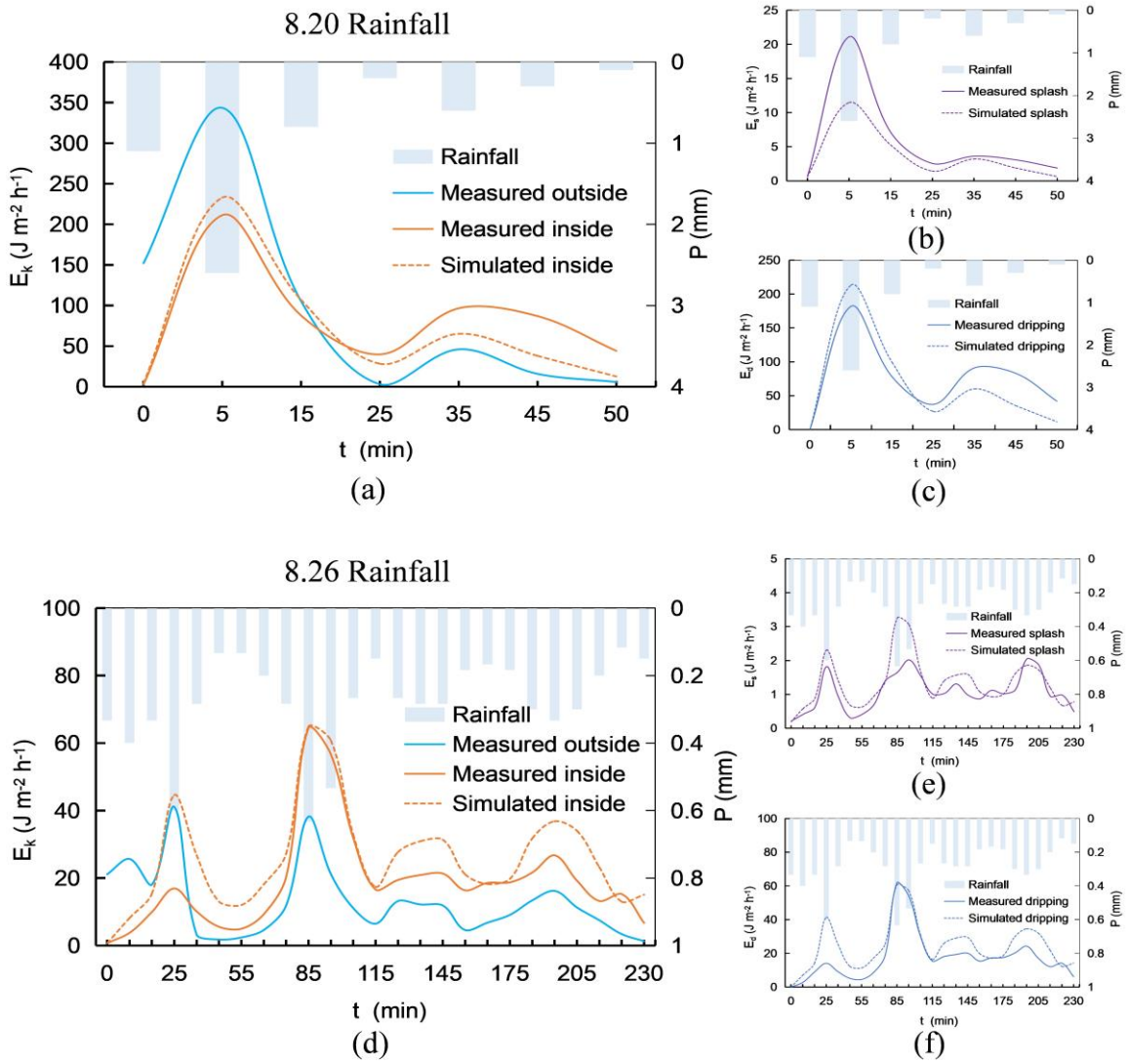

Figure 5. Comparison of kinetic energy of rainfall outside the canopy during two rainfall events (a) 8.20 total kinetic energy of rainfall (b) 8.20 kinetic energy of splashing drops under the canopy (c) 8.20 kinetic energy of dripping drops under the canopy (d) 8.26 total kinetic energy of rainfall (e) 8.26 kinetic energy of splashing drops under the canopy (f) 8.26 kinetic energy of dipping drops under the canopy.

Figure 5 shows a comparison between simulated and measured kinetic energy under anopy during two rainfall events. The overall trends of both are generally consistent, and the variations in kinetic energy are also in agreement with those observed outside the forest. However, the simulated splash kinetic energy shows a slightly greater discrepancy compared to the measured values. The complexity of the splash phenomenon, including the presence of larger splash drops not accounted for in the simulation triangular distribution assumption, may explain the discrepancy. However, since splash droplet kinetic energy constitutes a small fraction of the total kinetic energy (about 3%-10%), its impact on the total inside kinetic energy simulation is minimal.

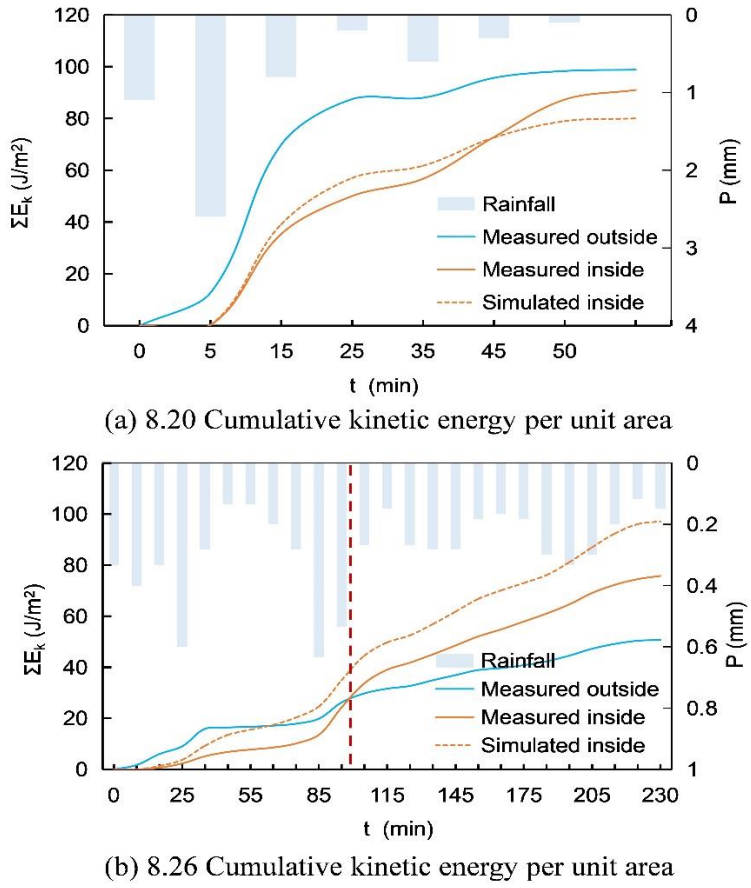

Figure 6. Cumulative kinetic energy per unit area. (a) 8.20 Rainfall event, (b) 8.26 Rainfall event.

Figure 6 compares measured and simulated cumulative kinetic energy per unit area in open versus sub-canopy conditions during two rainfall events. Initially, sub-canopy energy remains lower than open rainfall due to canopy interception. As the canopy approaches saturation, increased canopy dripping drives significant energy escalation beneath the canopy. In contrast, during the 26 August event, sub-canopy energy surpasses outside rainfall energy at t ≈ 100 min, ultimately reaching nearly twice the open-environment value. Thus, assessing the canopy impact on rainfall kinetic energy requires a comprehensive analysis of canopy leaf inclination, contact angle, branch height, interception volume and the external raindrop spectrum to determine whether the kinetic energy beneath the canopy is greater or less than that outside. Smaller branch heights and larger leaf inclination angles may result in smaller and slower canopy drip, potentially leading to lower kinetic energy under the canopy.

3.3 Sensitivity Analysis

The uncertainties and influences associated with external factors, the threshold values used for measured component partitioning, typical model parameters, the determination of falling height and canopy traits are analyzed in this section, which can be seen in Figures 7-9 and Table 5. In the sensitivity analysis, only the parameter of interest was

varied, while all other parameters were kept at the values listed in Table 2.

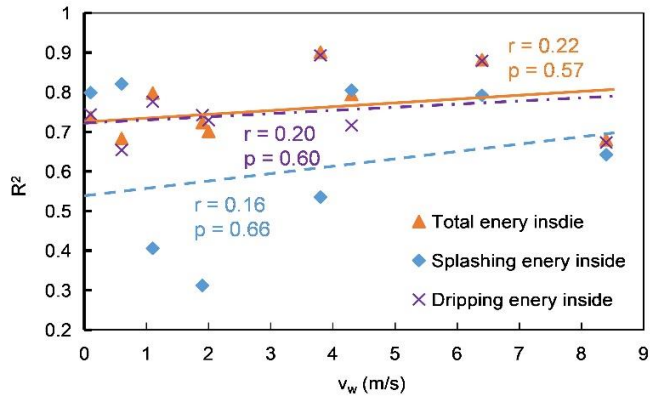

(a) The relationship between R^2 and wind speed (m/s)

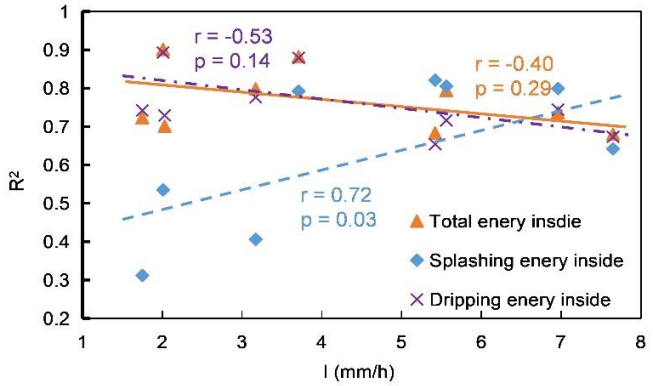

(b) The relationship between R^2 and rainfall intensity (mm/h)

Figure 7. Sensitivity Analysis Between Model Metric R^2 and External Influencing Factors: (a) Wind Speed, (b) Rainfall Intensity. r is Correlation coefficient, and p-value indicates the significance of the linear relationship from the t-test (p<0.05 is significant).

Since the RMSE metric is influenced by the total kinetic energy outside the canopy, the R^2 metric was adopted for the sensitivity analysis of external influencing factors of wind speed and rainfall intensity, as shown in Figure 4. Figure 4 (a) indicates that wind load has no significant effect on model performance, with p-values consistently above 0.5. This likely occurs because the estimation of under-canopy raindrop size distribution accounts for wind load effects through the coefficient *k* (see Eqs (6) in Sect 2.2., and Li et al., 2025), maintaining relatively stable model performance across varying wind speeds. As mean rainfall intensity increases, the performance for total kinetic energy and dripping kinetic energy shows a declining trend, while splashing kinetic energy exhibits an increasing trend. Notably, the simulation performance of splash kinetic energy increased significantly with increasing rainfall intensity ($p < 0.05$). This phenomenon is consistent with the observations of Nanko et al. (2025), who concluded that splash is predominantly driven by rainfall. This may be attributed to: (1) splashing being less pronounced at low rainfall intensities, leading to biased splashing energy estimates; and (2) significant leaf vibration induced by high

rainfall intensities, which is not currently considered in the model, resulting in slightly diminished performance in total and dripping energy with increasing rainfall intensity.

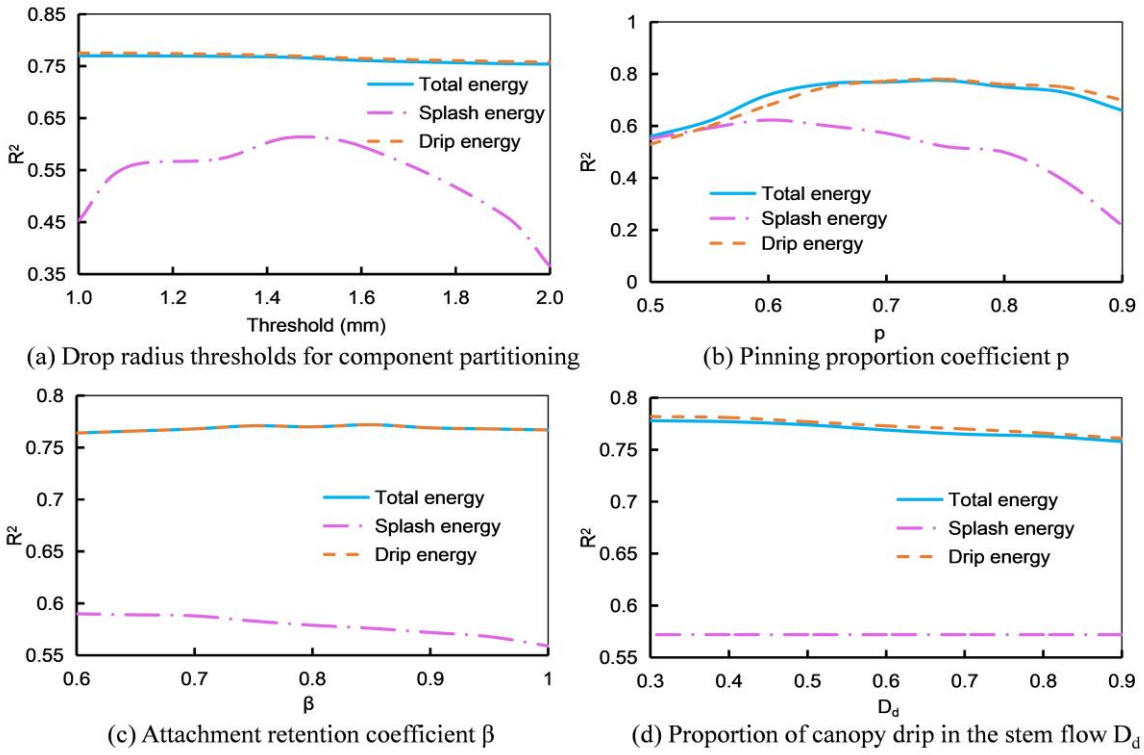

Figure 8. Sensitivity Analysis of the threshold values and typical model parameters. The R^2 is computed as an overall metric by concatenating all nine events. (a) Drop radius thresholds for component partitioning; (b) Pinning proportion coefficient p; (c) Attachment retention coefficient β; (d) Proportion of canopy drip in the stem flow D_d

As shown in Figure 8(a), the experimentally measured component partitioning thresholds were relatively stable between 1.1 and 1.6 mm, with R^2 fluctuating between 0.55 and 0.65. Thresholds below 1.1 mm or above 1.6 mm resulted in noticeable decreases. The drip kinetic energy and total kinetic energy were not sensitive to this threshold. Figure 4 also shows that the volume fraction of raindrops between 1 and 2 mm is relatively small, as most drip drops are larger than 2 mm and most splash drops are smaller than 1 mm; the contribution from 1–2 mm drops may mainly correspond to free throughfall. Therefore, selecting 1.3 mm as the experimentally measured threshold for analysis is appropriate.

As shown in Figures 4(b-d), the model is most sensitive to the parameter p, which is defined as the proportion of volume remaining on the leaf or stem after splashing. This is also evident from Eqs (11) and (12), where p, as an external multiplicative factor, has a direct and substantial impact, while the parameters β and D_d affect only specific terms. Physically, the value of p is related to factors such as rainfall intensity and leaf surface properties, and further investigation is needed to better understand its behavior.

Table 5. Sensitivity analysis of two methods for calculating falling height: the average height of the lowest canopy layer versus

the actual height distribution

Metrics	Splash	Drip	Total
Correlation Index (r)	1.000	0.999	0.999
p value form Paired t-test	0.97	0.91	0.91
Mean Relative Error (MRE) (h distribution as the denominator)	0.1%	1.6%	1.6%

Note：All metrics were calculated based on the concatenation of the nine rainfall events into a single continuous time series.

Through sensitivity analysis in Table 5, it was found that using the height distribution shown in Figure 3(b) for simulation versus using the average height resulted in very minor differences in this case. The mean deviation of splash kinetic energy was only 0.1%, while deviations for drip kinetic energy and total kinetic energy were approximately 1.6%, with correlation coefficients all exceeding 0.999, indicating no significant differences. The likely reason is that for this tree species, the branch height is relatively large (>4 m), so most raindrops reach over 90% of their terminal velocity. In addition, due to the relatively high leaf area density of the species, the height distribution is concentrated, mostly between 4.7 and 5.1 m, resulting in a narrow distribution.

To further examine the influence of canopy traits on the model results, the percentage changes in the event-averaged kinetic energy across the nine rainfall events were plotted, using the parameters in Table 2 as the baseline.

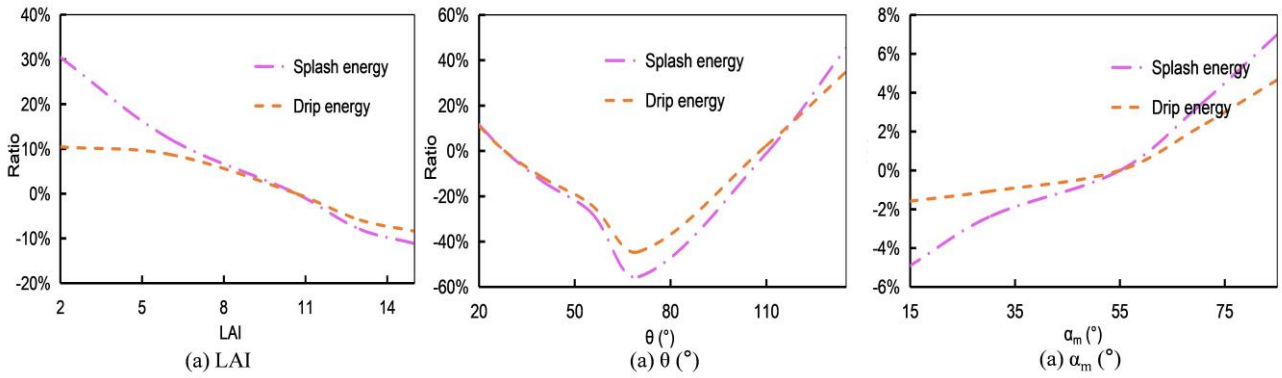

Figure 9. Sensitivity Analysis of the canopy traits. The vertical axis shows the percentage deviation from the baseline parameters (Table 2). (a) LAI; (b) θ (°); (c) Mean leaf inclination angle α_m (°).

Figure 9 indicates that the estimated kinetic energy decreases monotonically with increasing LAI; exhibits a decrease followed by an increase as θ increases; and increases with increasing α_m. Sensitivity analysis further shows that the model is most responsive to variations in θ, followed by LAI and, to a lesser extent, α_m. The observed increase in sub-canopy kinetic energy corresponds to the reduction in canopy interception volume, which is consistent with the underlying physical processes.

4. Discussion

The purpose of this model is to quantitatively estimate the kinetic energy of splash, drip, and free throughfall beneath the canopy during rainfall events based on the canopy structural parameters and physically meaningful model parameters listed in Table 2. For different tree species, model parameters such as p, D_d, and β may either adopt the typical values listed in Table 2 or be recalibrated based on new experimental observations. The kinetic energy estimated by the model can further serve as an input to soil-erosion computation models and related applications. However, several limitations and potential improvements related to model assumptions remain.

First, the influence of branch drip has not been fully considered. The model uses parameters such as Dd and pt to represent the proportions of stem drip and splash, and it assumes that the size distributions of branch-generated drip and splash droplets are the same as those from leaves. This assumption may introduce biases, as Nanko et al. (2022) reported that branch drip points can generate larger droplets, which substantially affect kinetic energy. Nevertheless, because the observations in this study were conducted during summer when foliage is dominant, the effect of branch drip points was less pronounced. Future work could further refine the representation of branch drip in the model.

Second, the assumptions used for component partitioning in the model are relatively simplified. For computational convenience, the volume distribution of splash droplets is assumed to follow a triangular distribution between 0.3 and 1.3 mm, based on the Weibull distribution curve proposed by Levia et al. (2019). However, this assumption neglects splash droplets in the 1.3-2 mm range, although their proportion is small, which introduces additional error.

Third, several aspects of the experimental measurements can also be further improved. These include the measurement uncertainty introduced by the 32-bin discretization of diameter and velocity in the laser spectrometer; the use of a fixed radius threshold to partition measured components, which, despite the sensitivity analysis shown in Figure 8(a), still leaves room for refinement; and the limited scope of observations, which are restricted to nine rainfall events on a single tree species. Future work could expand measurements to different species and seasons to support deeper model evaluation and improvement.

5. Summary

Based on the research of Li and Tian (2025), this study established the new rainfall kinetic energy under canopy estimation model, combined with high-precision LiDAR data to obtain canopy physical parameters, and used nine field rainfall experimental observations to verify and analyze the model simulation results. The analysis led to the following conclusions:

1. The introduction of splash and canopy drip mechanisms into canopy interception modeling, enhanced by LiDAR-derived structural parameters, enables simulation of sub-canopy raindrop spectra and kinetic energy during rainfall events. This approach shows preliminary potential for soil erosion studies, though further validation with expanded datasets is required given current limitations to nine rainfall events.

2. The model simulations indicate that the sub-canopy raindrop spectrum and rainfall kinetic energy are primarily governed by canopy physical properties such as interception intensity, splash retention, and leaf inclination, and thus remain relatively stable when these properties are unchanged, regardless of variations in the above-canopy rainfall spectrum.

3. The sensitivity analysis indicates that the model is generally stable under most structural and observational assumptions. Rainfall intensity and the pinning-proportion coefficient p remain the dominant controls, while other factors such as wind load, the partitioning threshold, and the falling-height method exert only minor influence. In addition, the parameters describing canopy traits introduce additional variability, with $\boldsymbol{\theta}$ showing the highest sensitivity, followed by LAI and $\boldsymbol{\alpha_m}$.

Overall, the model's current limitations, particularly the simplified treatment of branch drip, the assumptions used for component partitioning, and the measurement uncertainties inherent in observations, highlight the need for future work that incorporates improved parameterization, refined observational methods, and expanded experiments across different species and seasons.

Notation

Rainfall and Kinetic Energy of Rainfall

E_d Drip kinetic energy per unit area per unit time (J m^{-2} h^{-1})

E_{Kp} Kinetic energy per unit area unit rainfall depth (J m^{-2} mm^{-1})

E_{K_in} Kinetic energy per unit area per unit time inside the canopy (J m^{-2} h^{-1})

E_{K_out} Kinetic energy per unit area per unit time outside the canopy (J m^{-2} h^{-1})

$E(D)$ Kinetic energy of a single droplet (J)

P Rainfall amount (mm)

I Rainfall intensity (mm/h)

I' Rainfall intensity reaching the last canopy layer (mm/h)

E_s Splash kinetic energy per unit area per unit time (J m^{-2} h^{-1})

E_{K_total} Total kinetic energy (J)

E_K Total kinetic energy of rainfall per unit area per unit time (J m^{-2} h^{-1})

Canopy

γ Fractional Vegetation Cover (FVC)

LAI Leaf area index

G Leaf area projection ratio

SAI Stem area index

α Leaf inclination angle

Y Leaf interception capacity (mm)

K_l Leaf interception coefficient

w_l Leaf interception volume (mm)

α_m Mean leaf inclination angle

K_s Stem interception coefficient

w_s Stem interception volume (mm)

S Stem interception capacity (mm)

p_t Stem area ratio

Physics

β Attachment retention coefficient

θ Average of the advancing and retreating contact angles on the leaf surface

ρ Density of water (kg/m^3)

m_a Dripping mass per unit area per unit time (kg m^{-2}s^{-1})

v_a Dripping droplet velocity (m/s)

A Drop spectrometer observation area (cm^2)

t_0 Drop spectrometer observation time (h)

V Droplet volume (mm3)

v_0 Fall velocity of the droplet (m/s)

h Falling height of the droplets (m)

v Final velocity of the droplet (m/s)

X Half of the difference between the advancing and receding contact angles

e_{pl} Leaf evaporation intensity (mm/h)

s_{max} Maximum radius of the droplet contact surface (mm)

p Pinning proportion coefficient

D_d Proportion of canopy drip in the stem flow

s Radius of the droplet contact surface (mm)

t Rainfall duration (h)

v_s Splash droplet velocity (m/s)

m_s Splash mass per unit area per unit time (kg m^{-2}s^{-1})

e_{ps} Stem evaporation intensity (mm/h)

σ Surface tension coefficient of water (N/m)

k_s Volumetric portion of leaf and stem splash drops

k_a Volumetric portion of canopy drip including leaf and stem drip

D Waterdrop diameter (mm)

$v_{\_in}$ Waterdrop velocity inside the canopy (m/s)

k Wind load effect coefficient

v_w Wind speed (m/s)

Data Available Statement

The data used in the study, such as raindrop spectrum observations, data of rainfall kinetic energy, and model running python code are available at Zenodo (Li, 2025).

Acknowledgments

This study has been supported by the National Natural Science Foundation of China (U2442201 & 523B1006), and the National Key Research and Development Program of China (2022YFC3002900).

References

Alivio, M. B., Bezak, N., and Mikoš, M.: The size distribution metrics and kinetic energy of raindrops above and below an isolated tree canopy in urban environment, Urban For. Urban Greening, 85, 127971, doi:10.1016/j.ufug.2023.127971, 2023.

Atlas, D., Srivastava, R. C., and Sekhon, R. S.: Doppler radar characteristics of precipitation at vertical incidence. Rev. Geophys., 11(1), 1-35, doi: 10.1029/RG011i001p00001, 1973

Brasil, J. B., Andrade, E. M. D., Araújo de Queiroz Palácio, H., Fernández-Raga, M., Carvalho Ribeiro Filho, J., Medeiros, P. H. A., and Guerreiro, M. S.: Canopy effects on rainfall partition and throughfall drop size distribution in a tropical dry forest, ATMOSPHERE-BASEL, 13, 1126, doi:10.3390/atmos13071126, 2022.

Chen, C., Jia, Y., Zhang, J., Yang, L., Wang, Y., and Kang, F.: Development of a 3D point cloud reconstruction-based apple canopy liquid sedimentation model, J. Cleaner Prod., 451, 142038, doi:10.1016/j.jclepro.2024.142038, 2024.

de Moraes Frasson, R. P., and Krajewski, W. F.: Rainfall interception by maize canopy: Development and application of a process-based model, J. Hydrol., 489, 246–255, doi:10.1016/j.jhydrol.2013.03.019, 2013.

Du, S., Lindenbergh, R., Ledoux, H., Stoter, J., and Nan, L.: AdTree: Accurate, detailed, and automatic modelling of laser-scanned trees, Remote Sens., 11, 2074, doi:10.3390/rs11182074, 2019.

Fernández-Raga, M., Fraile, R., Keizer, J. J., Teijeiro, M. E. V., Castro, A., Palencia, C., and Marques, R. L. D. C.: The kinetic energy of rain measured with an optical disdrometer: An application to splash erosion, Atmos. Res.,

96, 225–240, doi:10.1016/j.atmosres.2009.07.013, 2010.

Gash, J. H. C., and Morton, A. J.: An application of the Rutter model to the estimation of the interception loss from Thetford forest, J. Hydrol., 38, 49–58, doi:10.1016/0022-1694(78)90131-2, 1978.

Geißler, C., Nadrowski, K., Kühn, P., Baruffol, M., and Bruelheide, H.: Kinetic Energy of Throughfall in Subtropical Forests of SE China – Effects of Tree Canopy Structure, Functional Traits, and Biodiversity, PLoS ONE, 8, e49618, doi:10.1371/journal.pone.0049618, 2013.

Hosoi, F., and Omasa, K.: Voxel-based 3-D modeling of individual trees for estimating leaf area density using high-resolution portable scanning lidar, IEEE Trans. Geosci. Remote Sens., 44, 3610–3618, doi:10.1109/TGRS.2006.881743, 2006.

Howard, M., Hathaway, J. M., Tirpak, R. A., Lisenbee, W. A., and Sims, S.: Quantifying urban tree canopy interception in the southeastern United States, Urban For. Urban Greening, 77, 127741, doi:10.1016/j.ufug.2022.127741, 2022.

Katayama, A., Nanko, K., Jeong, S., Kume, T., Shinohara, Y., and Seitz, S.: Concentrated impacts by tree canopy drips: Hotspots of soil erosion in forests, Earth Surf. Dyn. Discuss., 2023, doi:10.5194/esurf-11-1275-2023 1–12, 2023.

Konrad, W., Ebner, M., Traiser, C., and Roth-Nebelsick, A.: Leaf Surface Wettability and Implications for Drop Shedding and Evaporation from Forest Canopies, Pure Appl. Geophys., 169, 835–845, doi:10.1007/s00024-011-0330-2, 2012.

Levia, D. F., Carlyle-Moses, D., and Tanaka, T.: Forest hydrology and biogeochemistry: synthesis of past research and future directions, Springer Sci. Bus. Media, 216, 2011.

Levia, D. F., Hudson, S. A., Llorens, P., & Nanko, K.: Throughfall drop size distributions: a review and prospectus for future research. Wiley Interdiscip. Rev.: Water, 4(4), e1225, doi:10.1002/wat2.1225, 2017.

Levia, D. F., Nanko, K., Amasaki, H., Giambelluca, T. W., Hotta, N., Iida, S. I., ⋯& Yamada, K.: Throughfall partitioning by trees. Hydrol. Process., 33(12), 1698–1708, doi:10.1002/hyp.13432, 2019.

Li, G., Wan, L., Cui, M., Wu, B., and Zhou, J.: Influence of canopy interception and rainfall kinetic energy on soil erosion under forests, FORESTS, 10, 509, doi:10.3390/f10060509, 2019.

Li, Z.: The open data of "Derivation and validation of estimation model of rainfall kinetic energy under canopy", Zenodo, doi.org/10.5281/zenodo.15472339, 2025.

Li, Z., and Tian, F.: Derivation and validation of a theoretical canopy interception model based on raindrop microphysical processes, Water Resour. Res., 61, e2024WR038296, doi:10.1029/2024WR038296, 2025.

Li, Z., Tian, F., Wang, D., and Peng, Z.: A stochastic simulation method for estimating vegetation interception capacity based on mechanical-geometric analysis, Water Resour. Res., 61, e2025WR040267, doi:10.1029/2025WR040267, 2025.

Maćkiewicz, A., and Ratajczak, W.: Principal components analysis (PCA), Comput. Geosci., 19, 303–342, 1993.

Miralles, D. G., Gash, J. H., Holmes, T. R., de Jeu, R. A., and Dolman, A. J.: Global canopy interception from satellite observations, J. Geophys. Res. Atmos., 115, D16122, doi:10.1029/2009JD013530, 2010.

Momiyama, H., Kumagai, T. O., Fujime, N., Egusa, T., and Shimizu, T.: Forest canopy interception can reduce flood discharge: Inferences from model assumption analysis, J. Hydrol., 623, 129843, doi:10.1016/j.jhydrol.2023.129843, 2023.

Montero-Martinez, G., Garcia-Garcia, F., and Arenal-Casas, S.: The change of rainfall kinetic energy content with altitude, J. Hydrol., 584, 124685, doi:10.1016/j.jhydrol.2020.124685, 2020.

Mostafa, H., Saha, K. K., Tsoulias, N., and Zude-Sasse, M.: Using LiDAR technique and modified Community Land Model for calculating water interception of cherry tree canopy, Agric. Water Manag., 272, 107816, doi:10.1016/j.agwat.2022.

Mou, J.: Formula for calculating raindrop velocity, Chin. J. Soil Water Conserv., 3, 40–41, 1983.

Murakami, S.: Water and energy balance of canopy interception as evidence of splash droplet evaporation hypothesis, Hydrol. Sci. J., 66, 1248–1264, doi:10.1080/02626667.2021.1924378, 2021.

Nanko, K., Mizugaki, S., and Onda, Y.: Estimation of soil splash detachment rates on the forest floor of an unmanaged Japanese cypress plantation based on field measurements of throughfall drop sizes and velocities, Catena, 72, 348–360, doi:10.1016/j.catena.2007.07.002, 2008.

Nanko, K., Onda, Y., Ito, A., and Moriwaki, H.: Effect of canopy thickness and canopy saturation on the amount and kinetic energy of throughfall: An experimental approach, Geophys. Res. Lett., 35, L05402, doi:10.1029/2007GL033010, 2008.

Nanko, K., Watanabe, A., Hotta, N., and Suzuki, M.: Physical interpretation of the difference in drop size distributions of leaf drips among tree species, Agric. For. Meteorol., 169, 74–84, doi:10.1016/j.agrformet.2012.09.018, 2013.

Nanko, K., Keim, R. F., Hudson, S. A., & Levia, D. F.: Throughfall drop sizes suggest canopy flowpaths vary by phenophase. J. Hydrol., 612, 128144, doi:10.1016/j.jhydrol.2022.128144, 2022.

Nanko, K., Levia, D. F., Iida, S. I., Shinohara, Y., & Sakai, N.: Machine learning reveals the contrasting roles of rainfall and canopy structure metrics on the formation of canopy drip and splash throughfall. J. Geophys. Res.: Biogeosci., 130(2), e2024JG008340, doi:10.1029/2024JG008340, 2025.

Pflug, S., Voortman, B. R., Cornelissen, J. H., and Witte, J. P. M.: The effect of plant size and branch traits on rainfall interception of 10 temperate tree species, Ecohydrology, 14, e2349, doi:10.1002/eco.2349, 2021.

Rutter, A. J., Kershaw, K. A., Robins, P. C., and Morton, A. J.: A predictive model of rainfall interception in forests, 1. Derivation of the model from observations in a plantation of Corsican pine, Agric. Meteorol., 9, 367–384, doi:10.1016/0002-1571(71)90034-3, 1971.

Senn, J. A., Fassnacht, F. E., Eichel, J., Seitz, S., and Schmidtlein, S.: A new concept for estimating the influence of vegetation on throughfall kinetic energy using aerial laser scanning, Earth Surf. Processes Landforms, 45, 1487–1498, doi:10.1002/esp.4820, 2020.

Tu, L., Xiong, W., Wang, Y., Yu, P., Liu, Z., Han, X., and Xu, L.: Integrated effects of rainfall regime and canopy structure on interception loss: A comparative modelling analysis for an artificial larch forest, Ecohydrology, 14, e2283, doi:10.1002/eco.2283, 2021.

Valente, F., David, J. S., and Gash, J. H. C.: Modelling interception loss for two sparse eucalypt and pine forests in central Portugal using reformulated Rutter and Gash analytical models, J. Hydrol., 190, 141–162,

doi:10.1016/S0022-1694(96)03066-1, 1997.

Van Dijk, A. I. J. M., Bruijnzeel, L. A., and Rosewell, C. J.: Rainfall intensity–kinetic energy relationships: a critical literature appraisal, J. Hydrol., 261, 1–23, doi:10.1016/S0022-1694(02)00020-3, 2002.

Wang, S., Liu, C., Li, W., Jia, S., and Yue, H.: Hybrid model for estimating forest canopy heights using fused multimodal spaceborne LiDAR data and optical imagery, Int. J. Appl. Earth Obs. Geoinf., 122, 103431, doi:10.1016/j.jag.2023.103431, 2023.

Xiao, Q., McPherson, E. G., Ustin, S. L., and Grismer, M. E.: A new approach to modeling tree rainfall interception, J. Geophys. Res., 105, 29173–29188, doi:10.1029/2000JD900343, 2000.

Yao, W., and Chen, G.: Raindrop falling velocity and terminal velocity formula, J. Hohai Univ. Nat. Sci. Ed., 21, 21–27, 1993.

Zhang, R., Seki, K., and Wang, L.: Quantifying the contribution of meteorological factors and plant traits to canopy interception under maize cropland, Agric. Water Manag., 279, 108195, doi:10.1016/j.agwat.2023.108195, 2023.

Zhang, W., Liu, W., Li, W., Zhu, X., Chen, C., Zeng, H., and Yang, B.: Characteristics of throughfall kinetic energy under the banana (Musa nana Lour.) canopy: The role of leaf shapes, Catena, 197, 104985, doi:10.1016/j.catena.2020.104985, 2021.